CLM-P796

CLM-P796

UKAEA

Preprint

PREDICTIONS OF ELECTRON CYCLOTRON CURRENT DRIVE EFFICIENCY FOR A TOP-LAUNCHED EXTRAORDINARY MODE IN A TOKAMAK

R. O. DENDY
R. W. HARVEY
M. R. O'BRIEN

CULHAM LABORATORY
Abingdon, Oxfordshire
1987

CLM-P.796

PREDICTIONS OF ELECTRON CYCLOTRON CURRENT DRIVE EFFICIENCY FOR A TOP-LAUNCHED EXTRAORDINARY MODE IN A TOKAMAK

R.O Dendy, R.W. Harvey,[a] and M.R. O'Brien

Culham Laboratory, Abingdon, Oxon, OX14 3DB, England

(UKAEA/Euratom Fusion Association)

Abstract

A relativistic ray tracing code is used in conjunction with a Fokker-Planck code to calculate the dependence of current drive efficiency on plasma parameters and wave characteristics for top launch. Physical considerations include the interplay of wave polarisation, relativistic cyclotron resonance, optical path length, and electron collisionality. It is found that the current drive efficiency at a given temperature is a function of only two parameters: electron number density, and the parameter $\beta \equiv (\omega - \Omega_0)/k_{\parallel} v_B$, which includes information on magnetic field strength, wave launch angle, and plasma temperature. Peak current drive efficiencies can exceed by 25% the values for comparable inside launch configurations.

(Submitted for publication in Plasma Physics and Controlled Fusion)

[a] Permanent address: GA Technologies Inc., San Diego, CA 92138, USA.

November 1986

I. INTRODUCTION

The propagation and absorption of electromagnetic radiation in the electron cyclotron range of frequencies (ECRF) is the subject of extensive research in fusion plasma physics. Here, we consider an electron cyclotron resonance heating configuration that is of particular experimental and theoretical interest at present,[1-4] and examine its potential for current drive. The configuration involves launching ECRF waves from a position at the top of a tokamak towards the centre of the plasma, with a wavevector $\underline{k}$ which includes a component $k_{\parallel}$ parallel to the magnetic field direction. In general the extraordinary mode at the fundamental resonance is considered, although in the experiment of Ref. 1, the ordinary mode is employed. The wave frequency ω is significantly lower than the local cyclotron frequency Ω of the electrons in the tokamak magnetic field: $\Omega = \Omega_0/\gamma$, where $\Omega_0 = eB_0/m_0c$ and γ is the Lorentz factor. The choice $\omega < \Omega$ is necessary for accessibility, so that the low-density extraordinary mode cutoff can be avoided. In addition, the condition for resonant coupling of energy from the wave to an electron with velocity component $v_{\parallel}$ parallel to the magnetic field direction is

$$\omega - k_{\parallel} v_{\parallel} - \Omega = 0 \qquad (1)$$

Because of the launch configuration chosen, and the geometry of the tokamak magnetic field, the value of $\omega - \Omega$ does not change greatly over a ray path. Thus, by Eq. (1), only a relatively narrow range of values of $v_{\parallel}$ fall into resonance. In this paper, our primary aim is to examine the

extent to which this fact can be exploited in driving a current. The basic electron cyclotron current drive mechanism[5] is most favourable when there is selective heating of electrons with low collisionality, and hence high velocity. Accordingly, the launch configuration described above, where it should be possible to concentrate heating on electrons at the high $v_{\parallel}$ end of the thermal distribution, is particularly interesting. We note that the success of lower hybrid current drive arises in part from the high parallel velocity of the accelerated resonant electrons.[6] The configuration studied here offers related benefits for electron cyclotron current drive.

Previous studies of this configuration have concentrated on heating, and have not extended to current drive. In Ref. 2, which contains a detailed discussion of the fully relativistic dispersion relation, a large, hot, dense plasma of the type predicted for INTOR was considered. Here, the large number of energetic electrons is highly favourable, and strong absorption is predicted. A more recent study[4] has concluded that strong heating should also be expected for discharges already attainable on TFTR and PLT. Two experimental studies have been carried out on PLT,[1,4] both in satisfactory agreement with theory. In both experiments, the resonant wave coupling was to superthermal tail electrons, rather than the Maxwellian distributions that we consider in this paper. Typical power levels were rather low, not exceeding 50kW, because of experimental constraints. The first experiment[1] used the ordinary mode with $k_{\parallel} = 0$, so that current drive was not possible, and the value of $\Omega - \omega$ was so large that resonance took place with relativistic superthermal electrons having energies of several hundred keV. In the second experiment,[4] an obliquely

launched extraordinary mode wave was used. Electron cyclotron emission and X-ray data confirmed that there was good coupling of wave energy to an already existing superthermal tail.

The present study of current drive is intended to complement these previous studies of heating. Following Refs. 2 and 3, we employ a relativistic, three-dimensional ray tracing code[7] to compute the power deposition in real space and in velocity space. The electron velocity distribution is Maxwellian, and the plasma parameters and magnetic field geometry are appropriate to the DITE tokamak.[8] As the principles of ray tracing are well-known,[9-11] we shall not discuss them here. Our code implements the relativistic expressions for the dielectric tensor elements derived by Shkarofsky,[12] using the treatment suggested by Airoldi and Orefice.[13] The results of the ray tracing calculation are used in conjunction with a quasilinear Fokker-Planck code. This balances wave-induced diffusion against collisions to calculate the steady-state electron velocity distribution, which in turn supports a current which can be calculated.[14] The ratio of this current to the total ECRF power input gives the current drive efficiency. In Section II, we consider in outline the factors that affect the dependence of absorption and current drive on the plasma parameters and the characteristics of the wave. The numerical results are presented in Section III, and our conclusions in Section IV.

II. THEORETICAL CONSIDERATIONS AFFECTING ABSORPTION AND CURRENT DRIVE

The degree of absorption that an electron cyclotron wave undergoes in a given region of space is a function both of the form of the electron velocity distribution $f(v_\perp, v_\parallel)$ and of the local polarisation of the

wave. Let us consider first the wave polarisation. This will be affected both by warm plasma finite Larmor radius considerations because $\omega \simeq \Omega$, and by cold plasma considerations since $(\Omega - \omega)/\omega$ is not negligibly small. A combination of these effects will apply at each point on a ray.

For a wave launched in the extraordinary mode, it is primarily that proportion of the energy which is right circularly polarised that undergoes electron cyclotron absorption. A number of detailed calculations of this proportion can be found in the literature,[2,12,15-18] to which we refer for a more extensive analysis. The broad features of the polarisation arise as follows. We are concerned with the right circular polarisation ratio

$$R = (E_x - iE_y)/E_y \tag{2}$$

where x , y are orthogonal coordinates perpendicular to the magnetic field direction. By Eq. (16) of Ref. 15, warm plasma considerations for the extraordinary wave at $\omega \simeq \Omega$ lead to

$$R \simeq \left(\frac{\pi^{1/2}}{2} \frac{\omega_P^2}{\omega^2} \frac{c}{N_\parallel v_B}\right)^{-1} \tag{3}$$

at normal densities. Here $\omega_p = (4\pi n_0 e^{2}/m_0)^{1/2}$ is the electron plasma frequency, v_B is the electron thermal velocity, n_0 is the electron number density, and $N_\parallel = ck_\parallel/\omega$ is the component of the wave refractive index parallel to the magnetic field direction. It is clear from Eq. (3) that the right circularly polarised component of a wave is enhanced by low density, high temperature, and a wave propagation direction with a large

component parallel to the magnetic field. For completeness, we note that at very low densities such that $\omega_p^2/\Omega^2 < 2(v_B/c)N_\parallel$, R is independent of the electron number density rather than proportional to its inverse.

We shall be considering waves for which $(\Omega - \omega)/\omega$ is not negligibly small. In this case, as pointed out in Ref. 18, cold plasma polarisation effects may also play a role. For a cold plasma,

$$R = 1 - \frac{\Omega}{\omega} \frac{\omega_p^2}{\Omega^2 + \omega_p^2 - \omega^2} \tag{4}$$

Thus R becomes larger as the magnitude of $\Omega - \omega$ increases. For the launch configuration outlined in Section I, we expect a combination of the effects described in Eqs. (3) and (4). That is, strong right circular polarisation should be favoured by arrangements that combine low plasma densities, large $|N_\parallel|$, and large $\Omega - \omega$, subject to the experimental constraints.

The degree of absorption is also a function of the path length L of the ray through the plasma. This dependence is described by the optical depth of the plasma,

$$\tau = \int_0^L \alpha(\omega - \Omega, N_\parallel) d\ell \tag{5}$$

Here $\alpha(\omega - \Omega, N_\parallel)$ denotes the absorption coefficient. It follows from Eq. (5) that $\tau \sim L$, and for a top launch position with the wave characteristics indicated, L increases with $|N_\parallel|$. Thus, considerations of path length as well as of polarisation favour large

values of $|N_\parallel|$ for strong absorption, subject again to further constraints.

Let us now consider the wave-particle resonance condition, Eq.(1), which includes the correction to the electron cyclotron frequency which arises from the relativistic dependence of electron mass on velocity. A detailed discussion of the effects of this relativistic correction has been given in Ref. 19. We shall be dealing with a configuration where the parameter $2(\Omega_o - \omega)/\Omega_o$ has a value which typically exceeds 0.1. For a central plasma temperature of 1.5 keV, $(v_B/c)^2 \simeq 0.005$. This large difference in magnitude implies that the term $v_\perp^2/c^2$ in Eq. (2) of Ref. 19 plays a very minor role in our context. The resonance parabola described in Fig. 1 of Ref. 19 therefore leads to resonant parallel velocities which are almost independent of $v_\perp$, for the values of $\Omega_0 - \omega$ with which we shall be concerned. We therefore write the cyclotron resonance condition in the form

$$\omega - \Omega_0 + \frac{1}{2}\frac{v_\parallel^2}{c^2}\Omega_0 = k_\parallel v_\parallel \tag{6}$$

Let us define

$$\alpha = \frac{1}{2|N_\parallel|}\ \frac{\Omega_0}{\omega}\frac{v_B}{c} \tag{7}$$

$$\beta = (\omega - \Omega_0)/k_\parallel v_B \tag{8}$$

Note that β is the resonant parallel velocity in the nonrelativistic approximation, calculated in multiples of v_B. Recall that accessibility

conditions cause us to choose $\omega < \Omega_0$, so that it is convenient to have $k_\parallel < 0$, making β positive . Then for the case of interest, Eqs. (6), (7) and (8) give for resonance

$$\frac{v_\parallel}{v_B} = \frac{1}{2\alpha} \left[(1 + 4\alpha\beta)^{1/2} - 1\right] \tag{9}$$

It is clear from Eq. (9) that unless $\alpha << 1/4\beta$, relativistic corrections to the resonance condition will be significant. As an example, consider a case that we shall deal with numerically later. We take $\omega = 2\pi \times 60$ GHz, corresponding to the electron cyclotron frequency for a magnetic field strength of 21.4 kG; a magnetic field strength of 26.0 kG at the top launch position; a launch angle of 45° to the perpendicular, giving $N_\parallel \simeq 1/\sqrt{2}$; and a central electron temperature of 1.5 keV. These parameters correspond by Eqs. (7) and (8) to $\alpha = 0.066$ and $\beta = 4$, so that $1/4\beta = 0.063$. Then by Eq. (9), the resonant value of $v_\parallel$ is $3.3\ v_B$, to be compared to a nonrelativistic value of $\beta v_B = 4v_B$. In general, as we shall discuss, lower resonant velocities will lead to stronger absorption when $v_\parallel$ is a few times v_B .

Returning to Eq. (9), we see that for given β , the magnitude of the relativistic reduction in the resonant velocity relative to βv_B increases as α increases. By Eq. (7), it follows that relativistic effects should tend to enhance absorption when $|N_\parallel|$ is small and Ω/ω is large. In the experiment , $\Omega/\omega \simeq 1$ and exceeds unity only by amounts of order 0.1. However, the value of $|N_\parallel|$ is considerably more flexible. We conclude that for the configuration of interest, the

dominant relativistic effect will be to enhance absorption at low $|N_\parallel|$. From first principles, this effect should be rather strong. The value of $v_\parallel$ at resonance determines the values of $\partial f/\partial v_\perp$ and $\partial f/\partial v_\parallel$ when calculating the poles of the dielectric tensor elements, which determine absorption. Since $f(v_\perp, v_\parallel) \sim \exp\left(-(v_\parallel/v_B)^2\right)$, small changes in $v_\parallel$ will cause large changes in the magnitude of the absorption. The relativistic dependence of absorption on $N_\parallel$ thus runs counter to the polarisation and path length considerations, which favour large $|N_\parallel|$.

Finally, let us recall the intrinsic efficiency of the current drive process itself, as distinct from the absorption process that is necessary for current drive. Relatively simple considerations of the balance between wave-induced electron diffusion and collisions indicate[5,20,21] that the current drive efficiency $\eta_{CD} = J/P$, where J is the current density and P the absorbed wave power density, satisfies

$$\eta_{CD} \sim v_\parallel^2/n_0 \qquad (10)$$

Here n_0 denotes the average electron number density. For electron cyclotron current drive, the resonant velocity $v_\parallel$ in eq. (10) is given by Eqs. (7) to (9). Equation (10) indicates that the values of α and β, or equivalently $\Omega - \omega$ and $N_\parallel$, should be chosen to maximise $v_\parallel$, subject to the very strong constraints on these parameters which arise from absorption requirements that have already been discussed. Again, low electron densities n_0 are favoured.

The precise numerical balance of all the effects outlined in this Section is calculated in the fully relativistic three-dimensional ray

tracing code that was discussed in the previous Section. Our quasilinear Fokker-Planck code then enables us to calculate the efficiency of the current drive process associated with the electron cyclotron absorption.

III. RESULTS

We have investigated numerically the dependence of electron cyclotron current drive for a top launch position on the following parameters: magnetic field strength at the launch position B_L ; launch angle ϕ relative to the perpendicular to the magnetic field direction, and hence $|N_\parallel|$; and electron number density at the centre of the tokamak, $n_e(0)$, assuming a parabolic density profile. In addition, we have attempted to isolate the role played by relativity on the one hand, and polarisation and optical path length considerations on the other.

The poloidal projection of typical ray paths, whose curvature arises from toroidicity, is shown in Fig. 1. It can be seen that the spatial power deposition is strongly localised to a narrow region which is nearly vertical. It follows that heating is concentrated on electrons whose parallel velocities fall within a narrow range of values. Our primary aim is to examine the extent to which this fact can be exploited for current drive, in comparison to side launch configurations where a wider range of values of $v_\parallel$ is sampled.

In Figs. 2 and 3, the current drive efficiency is plotted as a function of the parameter β given by Eq. (8), for launch angles ϕ of 30° and 60° to the perpendicular. The graphs have as a fixed parameter

the central electron density $n_e(0)$, which takes values between 0.5 and 2.0×10^{13} cm^{-3} . These values are somewhat lower than those considered in previous theoretical studies of heating with this configuration in large tokamaks,[2,3] because we are concerned with current drive and with a medium-size tokamak. Throughout our treatment, the central plasma electron temperature is 1.5 keV. Density and temperature profiles are parabolic. Since ϕ takes different values for Figs. 2 and 3, the value of $N_\parallel$ also takes different, approximately constant, values in Figs. 2 and 3. It follows from Eq. (8) that in both Figures, different values of β represent different magnetic field strengths, which alter $(\omega - \Omega_0)$, at constant $N_\parallel$. We summarise the information contained in Figs. 2 and 3 as follows.

(1) The graphs are very similar. For all densities and both launch angles considered, current drive is most effective in the range $2 < \beta < 3.8$. Peak current drive occurs near $\beta = 3.5$ throughout, and efficiency falls very steeply for $\beta \geq 3.8$. It is convenient that, despite the large number of competing effects outlined in the preceding Section, current drive efficiency can be related so simply to the primary engineering parameters $(\omega - \Omega_0)$ and $N_\parallel$.

(2) The current drive efficiency scales as $1/n_e(0)$. This scaling follows Eq. (10), which is derived from collisionality considerations and makes no reference to the dependence of polarisation and hence absorption on density. It is interesting to note the extent to which collisionality effects dominate absorption effects at low densities. For $n_e(0) = 0.5 \times 10^{13}$cm^{-3}, we found that power absorption was typically ten to twenty

per cent less than for $n_e(0) = 0.75 \times 10^{13} cm^{-3}$ - these densities lie in the very low density regime where absorption increases with density. However, when $\beta = 2$, the ratio of the current drive efficiency for $n_e(0) = 0.5 \times 10^{13} cm^{-3}$ to that for $n_e(0) = 0.75 \times 10^{13} cm^{-3}$ is approximately $1.4 \simeq 0.75/0.5$. This is because the benefits of low collisionality at the lower density overcome the negative effects of lower absorption.

(3) The roles of relativity, polarisation, and collisionlity in determining the current drive efficiency can be seen by comparing the results for $\beta = 4$ when $\phi = 30°$ and $60°$, which are almost identical. Consider first absorption. From Eq. (9), the relativistically correct resonant value of $v_\parallel/v_B$ is 3.14 for $\phi = 30°$, and 3.36 for $\phi = 60°$; this favours $\phi = 30°$ for absorption. However, by Eq. (8), the value $\beta = 4$ corresponds to a larger value of $(\omega - \Omega_0)$ for $\phi = 60°$ than for $\phi = 30°$. Thus, the polarisation considerations outlined in Section II favour $\phi = 60°$, as does the optical path length. The balance of these counteracting effects on absorption is calculated in our code, which shows that absorption is stronger for $\phi = 30°$ than for $\phi = 60°$. The code then goes on to calculate the current drive efficiency. By Eq. (10), this favours the case with the higher resonant velocity - in this case $\phi = 60°$ - because of its lower collisionality. The code shows that this effect almost exactly cancels the higher absorption for $\phi = 30°$, so that the final current drive efficiencies are the same.

(4) We have examined these effects further by running the code in a nonrelativistic form. In this case, the resonant velocity is βv_B for both $\phi = 30°$ and $\phi = 60°$. Thus there is no enhancement of absorption for $\phi = 30°$ arising from the relativistic correction to the resonant

parallel velocity, so that the polarisation and optical path length considerations which favour $\phi = 60°$ for absorption are unopposed. The nonrelativistic code calculates that in this case, for example when $n_e(0) = 0.75 \times 10^{13} cm^{-3}$ and $\beta = 4$, absorption is three times greater for $\phi = 60°$ than for $\phi = 30°$. Since the value of $v_\parallel$ in Eq.(10) is the same in both cases, namely βv_B, the effect of collisionality is the same. Consequently, the factor of three excess in absorption for $\phi = 60°$ is carried over to the current drive efficiency. This wide discrepancy from the relativistic treatment, which gives equal current drive efficiencies, illustrates the central role played by relativity.

(5) For purposes of comparison, we have calculated the current drive efficiency of the extraordinary mode in an inside launch position, for the plasma parameters already considered. The central magnetic field strength is set at 24.0 kG, so that the cyclotron resonance is off-centre, as usual for the cases that we have considered. We find that the top launch configuration gives superior current drive efficiency in the range $1.5 \lesssim \beta \lesssim 3.8$, and this range is independent of the density. The maximum enhancement is typically 25% of the inside launch current drive efficiency, and this peak occurs for $3.3 \lesssim \beta \lesssim 3.6$. This enhancement is a reflection of the capacity of the top launch configuration to concentrate heating on regions of velocity space which are most favourable for current drive.

IV. CONCLUSIONS

The efficiency of electron cyclotron current drive using the

extraordinary mode from a top launch position on a tokamak has been investigated numerically. A relativistic ray tracing code was used to calculate absorption, and this information was used in a Fokker-Planck code to calculate the current drive efficiency. The final result arises from the interplay of four classes of physical consideration: wave polarisation, relativistic cyclotron resonance of the electrons with the wave, optical path length, and electron collisionality. Despite the complexity of the interaction of these effects, the numerical results are relatively straightforward. The current drive efficiency at a given plasma temperature is essentially determined by only two parameters. These are firstly the electron number density, for which the scaling is approximately $1/n_e(0)$ in the range $0.5 \times 10^{13}\text{cm}^{-3}$ to $2.0 \times 10^{13}\text{cm}^{-3}$ considered; and secondly $\beta = (\omega - \Omega_0)/k_\parallel v_B$, for which the functional dependence is shown in Figs 2 and 3. We note that β is a function of the magnetic field strength, which determines $(\omega - \Omega_0)$, of the initial wave launch angle, which determines $k_\parallel$, and of the plasma temperature, which determines the electron thermal velocity v_B. The peak current drive efficiency occurs in the range $3.5 \leqslant \beta \leqslant 3.8$. In this case, the heating is concentrated on energetically favourable electrons, so that the efficiency exceeds by 25% the value for comparable inside launch configurations.

There are two main practical conclusions to be drawn. First, top launch is an attractive configuration for fundamental extraordinary mode current drive with a Maxwellian electron velocity distribution. Second, our results here give quantitative confirmation of effects that have positive implications when we look ahead to non-Maxwellian distributions with a superthermal tail. Polarisation and optical path considerations will be similar to those described here. The high degree of absorption

that we have obtained for $\beta \simeq 3.5$, together with the well-established general capacity for strong absorption demonstrated by superthermal tails,[22-27] indicate that substantial absorption can be expected. By Eq. (10), the intrinsic efficiency of current drive at relatively high $v_{\parallel}$ should be better than that considered here. There are good prospects for achieving an electron cyclotron current drive configuration that has benefits analogous to those which favour lower hybrid current drive, by using a top launch position.

REFERENCES

[1] E. Mazzucato, P. Efthimion, and I. Fidone, Nucl. Fusion 25, 1681 (1985).

[2] I. Fidone, G. Giruzzi, V. Krivenski, L.F. Ziebell, and E. Mazzucato, Phys. Fluids 29, 803 (1986).

[3] E. Mazzucato, I. Fidone, G. Giruzzi, and V. Krivenski, Nucl. Fusion 26, 3 (1986).

[4] E. Mazzucato, I. Fidone, A. Cavallo, S. von Goeler, and H.Hsuan, Nucl. Fusion 26, 1165 (1986).

[5] N.J. Fisch and A.H. Boozer, Phys. Rev. Lett. 45, 720 (1980).

[6] W. Hooke, Plasma Phys. 26, 133 (1984).

[7] P.J. Fielding, private communication.

[8] J.W.M. Paul, K.B. Axon, J.Burt, A.D. Craig, S.K. Erents, S.J. Fielding, D.H.J. Goodall, R.D. Gill, R.S. Hemsworth, M. Hobby, J. Hugill, G.M. McCracken, A. Pospieszczyk, B.A. Powell, R. Prentice, G.W. Reid, P.E. Stott, D.D.R. Summers, and C.M. Wilson, Proc. Sixth Int. Conf. on Plasma Physics and Controlled Nuclear Fusion Research (International Atomic Energy Agency, Vienna, 1977), Vol. 2, p.269.

[9] S.Weinberg, Phys. Rev. 126, 1899 (1962).

[10] I.B. Bernstein, Phys. Fluids 18, 320 (1975).

[11] M. Brambilla and A. Cardinali, Plasma Phys. 24, 1187 (1982).

[12] I.P. Shkarofsky, Phys. Fluids 9, 561 (1966).

[13] A.C.Airoldi and A. Orefice, J. Plasma Phys. 27, 515 (1982).

[14] D.F.H. Start, M.R. O'Brien, and P.M.V. Grace, Plasma Phys. 25, 1431 (1983).

[15] I. Fidone, G. Granata, G. Ramponi, and R.L. Meyer, Phys. Fluids 21, 645 (1978).

[16] M. Bornatici, Joint Workshop on Electron Cyclotron Emission and Electron Cyclotron Resonance Heating, Culham Laboratory CLM-ECR (1980), p.1.

[17] M. Bornatici, R. Cano, O. De Barbieri, and F. Engelmann, Nucl. Fusion 23, 1153 (1983).

[18] I. Fidone, G. Giruzzi, and E. Mazzucato, Phys. Fluids 28, 1224 (1985).

[19] R.A. Cairns, J. Owen, and C.N. Lashmore-Davies, Phys. Fluids 26, 3475 (1983).

[20] J.G. Cordey, T. Edlington, and D.F.H. Start, Plasma Phys. 24, 73 (1982).

[21] J.G. Cordey, Plasma Phys. 26, 123 (1984).

[22] I.Fidone, G. Granata, and R.L. Meyer, Plasma Phys. 22, 261 (1980).

[23] I. Fidone, G. Giruzzi, G. Granata, and R.L. Meyer, Phys. Fluids 26, 3284 (1983).

[24] M. Bornatici, U. Ruffina, and E. Westerhof, Plasma Phys. 28, 629 (1986).

[25] A. Montes and R.O. Dendy, Phys. Fluids 29, 2988 (1986).

[26] A.Ando, K.Ogura, H.Tanaka, M.Iida, S.Ide, K.Oho, S.Ozaki, M.Nakamura, T.Cho, T.Maekawa, Y.Terumichi, and S.Tanaka, Phys. Rev.Lett. 26, 2180 (1986).

[27] R.O.Dendy, M.R.O'Brien, M.Cox, and D.F.H.Start, Nucl.Fusion 26, accepted for publication (1986).

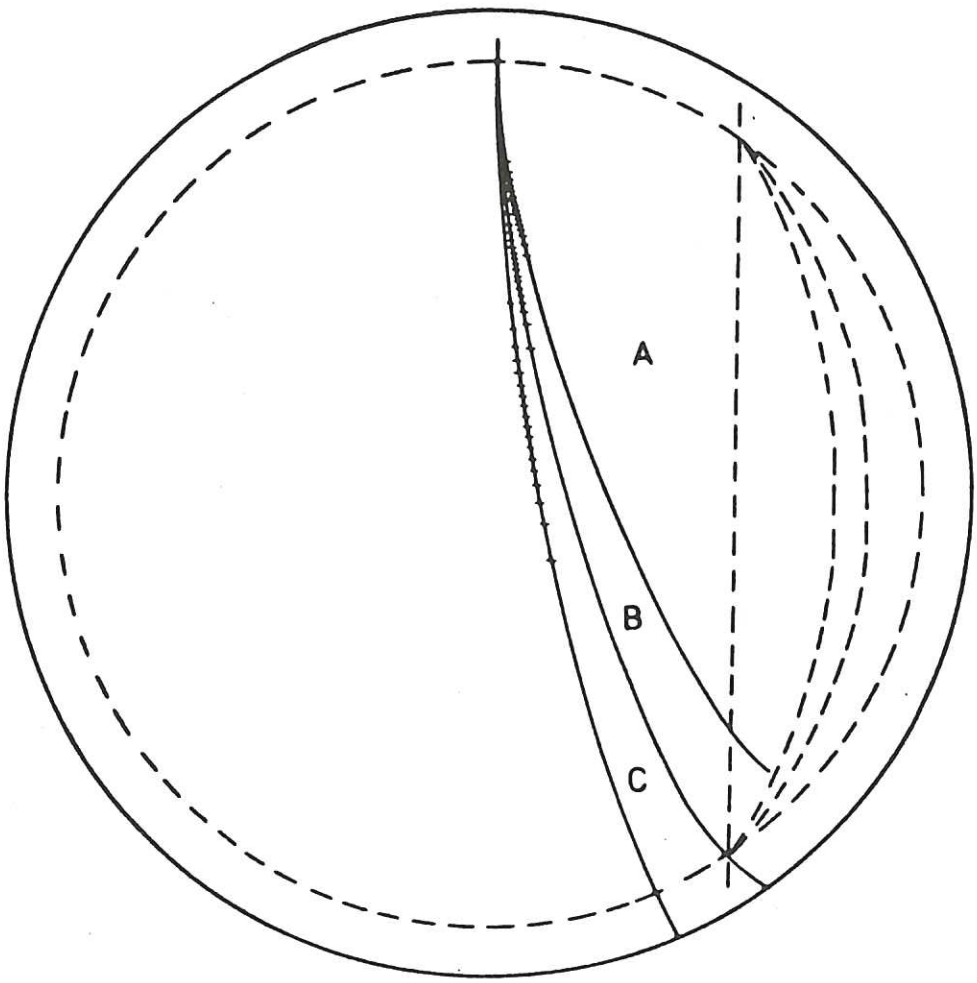

Fig. 1 Poloidal projection of ray paths. Launch angles ϕ measured from the perpendicular to the magnetic field direction are (a) $\phi=60°$, (b) $\phi=45°$, and (c) $\phi=30°$. Each cross on a ray marks a five per cent decrement in wave power. The vertical dashed line represents the fundamental electron cyclotron resonance for a 60 GHz source, and beyond it the upper hybrid resonance and low-density extraordinary mode cutoff are shown. Central magnetic field strength is 2.40 kG. Central electron density and temperature are $n_e(0)=1.0\times10^{13}\,cm^{-3}$ and $T_e(0)=1.5$ keV: parabolic profiles are assumed.

CLM-P796

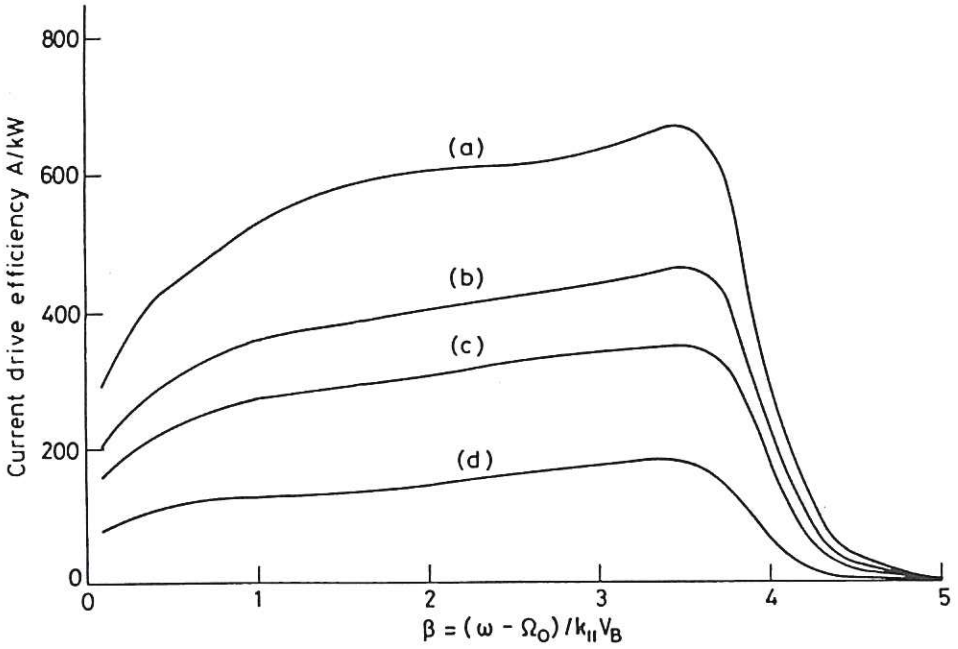

Fig. 2 Current drive efficiency as a function of the parameter $\beta=(\omega-\Omega_0)/k_{\|}V_B$ for a launch angle $\phi=30°$. Central electron densities $n_e(0)$ are: (a) $0.5\times10^{13}cm^{-3}$, (b) $0.75\times10^{13}cm^{-3}$, (c) $1.0\times10^{13}cm^{-3}$, (d) $2.0\times10^{13}cm^{-3}$.

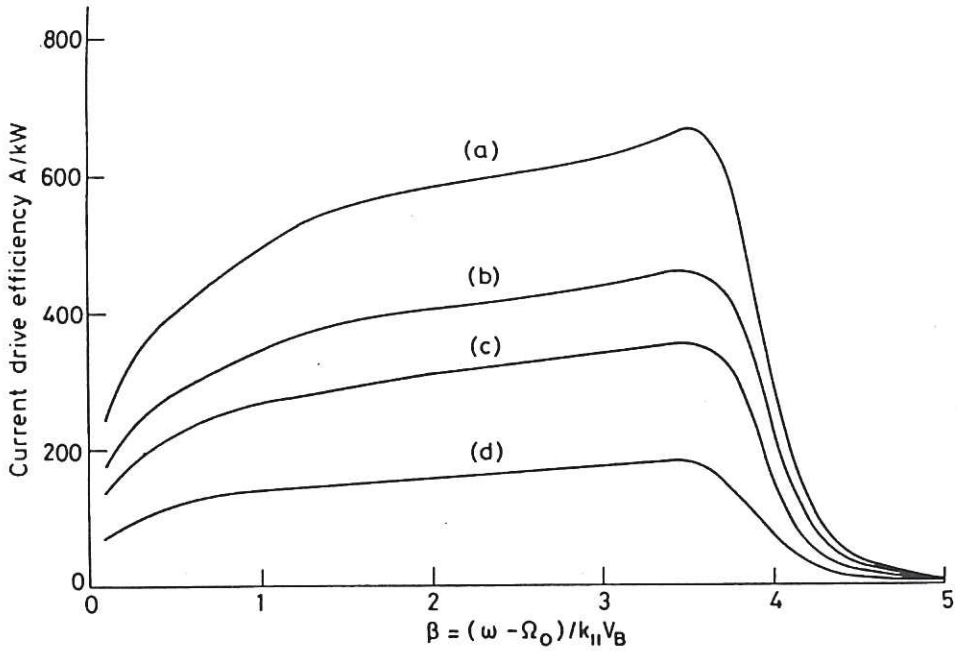

Fig. 3 Current drive efficiency as Fig. 2, for a launch angle $\phi=60°$.